Research Article | Open Access

Iontronics

Wang *et al. Iontronics* **2026**, *2*, 23 **DOI:**10.20517/iontronics.2026.011

Highly aligned bacterial cellulose/PPy gradient conductive membranes for directed cell differentiation under electrical stimulation

Li Wang[1,#], Fuyu Qi[1,#], Hao Wang[1,#], Sanming Hu[2], Shuangshuang Li[1], Zhijun Shi[1,*], Guang Yang[1,*]

Keywords:
Gradient conductive, topographical, electrical stimulation, aligned nanofiber, cell differentiation, peripheral nerve regeneration

Citation: Wang, L.; Qi, F.; Wang, H.; Hu, S.; Li, S.; Shi, Z.; Yang, G. Highly aligned bacterial cellulose/PPy gradient conductive membranes for directed cell differentiation under electrical stimulation. *Iontronics* **2026**, *2*, 23. https://dx.doi.org/10.20517/iontronics.2026.011

Received: 30 Mar 2026 **First Decision:** 11 May 2026 **Revised:** 24 May 2026 **Accepted:** 15 Jun 2026 **Published:** 8 Jul 2026

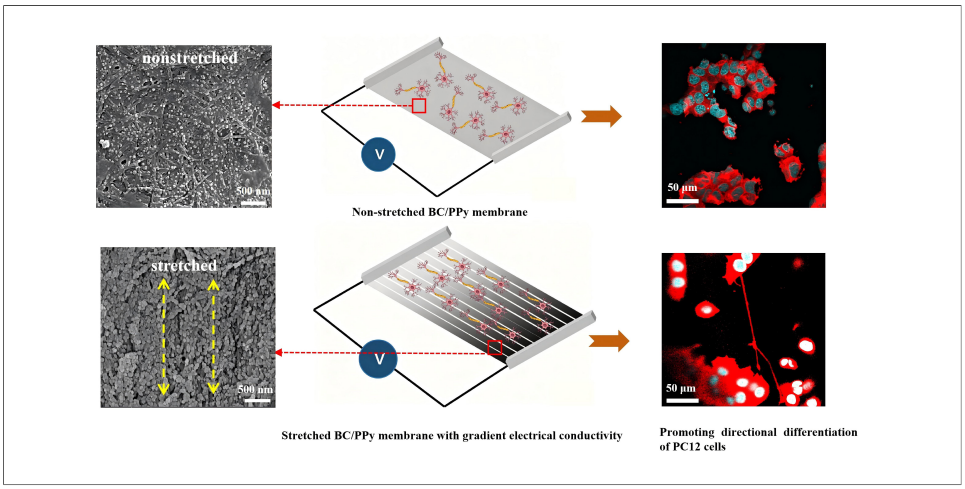

Abstract

Both topographical and gradient conductive cues can influence cellular activity and thereby affect tissue regeneration. However, their combined application on biomaterials together with electrical stimulation has not yet been demonstrated to achieve a synergistic effect. Herein, we hypothesized that a bacterial cellulose (BC)-based membrane incorporating aligned nanofibers and a concentration gradient of polypyrrole (PPy), when combined with electrical stimulation, would promote cell differentiation in peripheral nerve regeneration. The results showed that PPy was successfully deposited onto the aligned BC/PPy membrane with a gradient conductive structure. The resulting membrane exhibited good mechanical properties, thermal stability, a gradient decrease in surface resistance, a gradient increase in surface current from the upper to lower segments, and excellent biocompatibility. Notably, the membrane promoted gradient proliferation and differentiation of PC12 cells in vitro. Importantly, when combined with an applied electric field (EF), the aligned BC/PPy gradient conductive membranes synergistically directed the differentiation of PC12 cells. These findings suggest that aligned BC/PPy

[1]Department of Biomedical Engineering, College of Life Science and Technology, Huazhong University of Science and Technology, Wuhan 430074, Hubei, China,
[2]School of Biomedical Engineering and Imaging, Xianning Medical College, Hubei University of Science and Technology, Xianning 437100, Hubei, China
[#]These authors contributed equally to this work.

Correspondence to: Prof. Guang Yang, Prof. Zhijun Shi, Department of Biomedical Engineering, College of Life Science and Technology, Huazhong University of Science and Technology, Wuhan 430074, Hubei, China. E-mail: gyang-hust@hust.edu.cn; shizhijun@hust.edu.cn

gradient-conductive membranes, combined with EF, represent a promising therapeutic strategy for guiding cellular activities in peripheral nerve regeneration.

INTRODUCTION

Directional cell differentiation is critical for peripheral nerve regeneration[1], particularly in cases of long-distance or chronic nerve defects. Impaired cellular activity and uncontrolled neuronal differentiation may result in a functional gap between regenerated and native nerves, thereby hindering successful nerve repair. Currently, although autologous nerve grafting remains the gold standard for repairing peripheral nerve defects, it is associated with several limitations, including limited tissue availability, mismatched nerve diameters, donor-site morbidity, and loss of function[2,3]. Commercially available artificial substitutes are primarily used for repairing short-distance nerve gaps or as protective wrap devices[4]. However, they often rely on a single material and face challenges in mimicking the complex anatomical structure, as well as in achieving precisely guided cell differentiation and axonal reinnervation[5,6]. Therefore, there is a need to develop a novel strategy capable of programmatically directing the oriented growth, proliferation, and differentiation of cells at specific sites to promote accelerated peripheral nerve regeneration.

Biomaterials with aligned nanofibers have been demonstrated to effectively guide the oriented growth of neural cells and neurites, facilitating neurite extension across injured nerve gaps toward target tissues, thereby promoting nerve regeneration and functional recovery[7]. Bacterial cellulose (BC), a natural polymer produced by *Gluconacetobacter xylinus*, has recently received enormous attention due to its high mechanical strength, flexibility, and non-immunogenicity[8]. In particular, aligned BC nanofibers can provide contact guidance for directional neural stem cell elongation, neurite outgrowth[1], pheochromocytoma (PC12) cell differentiation, and Schwann cell migration along the nanofiber alignment[9]. Alternative methods for producing aligned cellulose often lead to reduced yield and disruption of the original BC structure[10]. To address this, our group successfully prepared highly aligned BC-based membranes via quantitative stretching, which exhibited excellent mechanical properties, biocompatibility, and guidance of cellular activities[11]. However, these aligned BC nanofibers lack electrical conductivity and thus cannot deliver electrical or electrochemical stimulation to nerve cells[12].

To render scaffolds conductive, the incorporation of polymeric or metallic conductive nanoparticles onto aligned fibers has been widely employed. Among these, polypyrrole (PPy) has been extensively studied for nerve regeneration due to its excellent electrical properties, good biocompatibility, and ease of synthesis[13,14]. For instance, Liu *et al.* reported that conductive polylactic acid/reduced graphene oxide/PPy composite nanofibers, when coupled with an electric field (EF), significantly accelerated PC12 cell proliferation and differentiation[15]. Similarly, Sun *et al.* developed a self-powered electrical stimulation system using Pt-BC/PPy-N-CNTs for nerve regeneration[16]. However, these scaffolds lack the ability to provide directional cues for cellular activities and axon growth during nerve repair. To enhance guidance capability, compositional gradients, which enable cells to infer their spatial location and determine their fate accordingly, have been applied in the design of new nerve conduits[17]. It has been reported that at the tip of the axon, growth cones can sense gradient guidance cues and modify their morphology to guide axon extension responsively[18]. Previous studies have shown that introducing growth factor or peptide gradient onto conduits can promote neurite extension and accelerate sciatic nerve regeneration[19,20]. In another study, the middle region of a gradient NGF-immobilized film achieved longer dorsal root ganglia (DRG) neurite outgrowth compared to films without an NGF gradient[21]. Nevertheless, a scaffold having both aligned nanofibers and a conductive PPy gradient has not yet been evaluated, nor its effects on cellular activities for nerve regeneration. To date, various methods have been developed for preparing gradient material, including electrospinning[22], 3D printing[23], and directional diffusion[19]. However, these approaches often involve

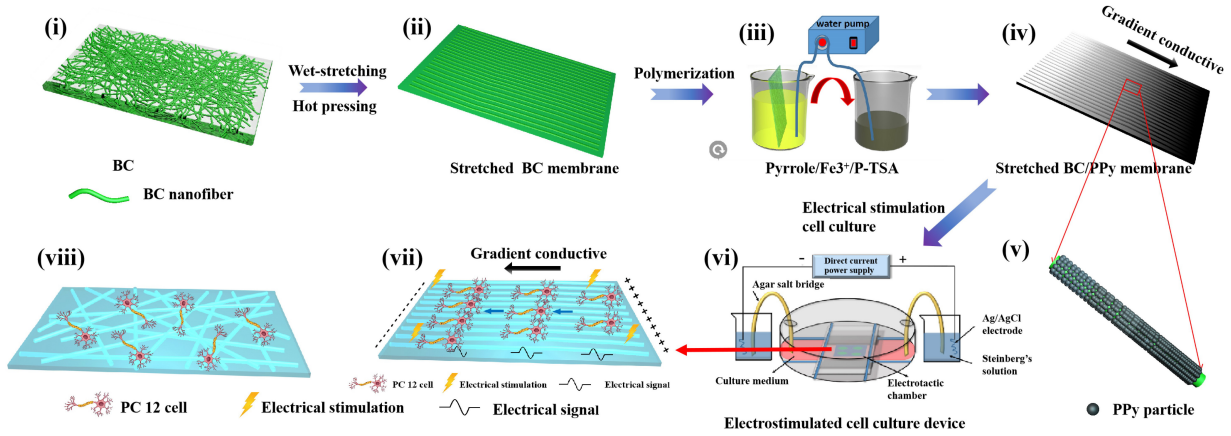

Figure 1. Schematic illustration of the preparation process for BC/PPy gradient conductive membranes and the electrotaxis chamber setup. The BC/PPy gradient conductive membranes were fabricated via a kinetically controlled reaction using a peristaltic pump. Subsequently, PC12 cells were seeded onto the membranes and subjected to electrical stimulation within an electrostimulation cell culture device. BC: Bacterial cellulose; PPy: polypyrrole; p-TSA: para-methylbenzenesulfonic acid; PC12: pheochromocytoma.

complex design requirements and challenging operation. Considering that aligned BC nanofibers allow the *in situ* polymerization of PPy onto their matrix, a time-controlled reaction method offers a simpler alternative, in which loading time serves as a key controlling parameter.

Endogenous EF can be detected at the injured nerve section and plays an important role in directing cellular activities during nerve regeneration[24]. However, the prolonged period required for nerve regeneration after injury may lead to target organ dysfunction or loss[15,25]. To mimic and sustain the effects of endogenous EF, exogenous electrical stimulation has emerged as a unique and promising treatment strategy for various types of peripheral nerve injury, including long-distance defects[6]. EF stimulation has been shown to promote the differentiation and proliferation of PC12 cells and axon extension[26]; it also increases intraneuronal cAMP levels in DRGs and NGF expression in Schwann cells[6]. Besides, EF can induce microtubule-associated proteins in axons, promote blood vessel regeneration, and thereby facilitate peripheral nerve regeneration[6]. Therefore, the combination of EF with a scaffold that provides both topographical guidance and gradient conductive signals may represent a novel approach for peripheral nerve regeneration. Recent studies have confirmed that gradient conductive scaffolds combined with oriented electrical stimulation can synergistically enhance nerve regeneration[27], and the integration of multilevel physicochemical cues has also shown promising prospects[28]. However, these strategies have not yet been implemented in the oriented BC/PPy system.

Herein, we developed a new nerve regeneration system that combined electrical cues with topographic and gradient conductive guidance of the BC/PPy gradient-conductive membranes for enhanced cell differentiation in peripheral nerve regeneration. The aligned BC/PPy gradient conductive membranes were first prepared by a quantitative stretching technique and hot pressing, followed by the introduction of gradient PPy along the nanofibers by a kinetically controlled reaction [Figure 1]. The physicochemical properties of the prepared gradient conductive membranes were systematically characterized in terms of morphology, chemical structures, electrical conductivity, and mechanical strength. Additionally, the biocompatibility and cell morphology on the aligned BC/PPy gradient conductive membranes were evaluated. Furthermore, the synergistic effect of coupling EF with the gradient conductive membranes on cell differentiation was investigated.

EXPERIMENTAL

Materials

BC was purchased from Hainan Guangyu Biotechnology Co., Ltd. (Hainan, China). Pyrrole (py) was obtained from Sigma-Aldrich (USA). Ferric chloride hexahydrate ($FeCl_3·6H_2O$) and para-methylbenzenesulfonic acid (p-TSA) were purchased from Sinopharm Chemical Reagent Co., Ltd (Shanghai, China). Dulbecco's modified eagle's medium (DMEM), Roswell Park Memorial Institute (RPMI) 1640, fetal bovine serum (FBS), horse serum, bovine serum albumin (BSA), penicillin/streptomycin (P/S), 3- (4,5-dimethylthiazol-2-yl)-2,5-diphenyltetrazolium bromide (MTT), and dimethylsul-foxide (DMSO) were acquired from Gibico Life Technologies Co., Ltd (Grand Island, USA). Anti-beta III tubulin monoclonal antibody and rhodamine-conjugated goat anti-mouse Immunoglobulin G (IgG) (H+L) secondary antibody were obtained from Proteintech Group, Inc. (USA). Dihydrochloride (DAPI), FITC-conjugated phalloidin, and Calcein-AM/PI were purchased from Dojindo Laboratories (Kyushu, Japan). Nerve growth factor (NGF) was acquired from Beijing Yiqiao Shenzhou Technology Co., Ltd. (China). Fluorescein isothiocyanate (FITC)-PC12 cells were generously provided by Huazhong University of Science and Technology (Wuhan, China). Sheep whole blood was purchased from Beijing Solarbio Technology Co., Ltd (Beijing, China).

Preparation of BC/PPy gradient conductive membranes

BC was purified by boiling in 0.1 M NaOH for 30 min, followed by washing with deionized water. The purified BC was then cut into pieces measuring 12 cm × 4 cm and wet-drawn at a speed of 1 mm/min until a stretching strain of 40% was reached. Subsequently, both the pristine and stretched BC membranes were hot-pressed at 100 °C for 12 h, as previously described[11].

The non-stretched and stretched BC/PPy gradient conductive membranes were fabricated by a kinetically controlled reaction using a peristaltic pump. First, a pyrrole solution containing 4.13 g of p-TSA and 1.61 g of pyrrole in 300 mL of water was slowly poured into a $FeCl_3$ solution (15.6 g of $FeCl_3·6H_2O$ in 300 mL of water) under gentle stirring to obtain the reaction mixture. When the solution turned black, the BC membranes were vertically immersed until fully submerged to the top segment. The peristaltic pump was then activated to withdraw the reaction solution at flow rates of 10, 20, and 30 mL/min, respectively. After completion of the reaction, the membranes were washed three times with deionized water and dried for 20 min to obtain the non-stretched BC/PPy gradient conductive membranes. Based on biocompatibility evaluation results, a flow rate of 20 mL/min was selected to control the reaction time for PPy gradient deposition on the membranes. The stretched BC/PPy gradient conductive membranes were prepared following the same procedure.

Characterization of BC/PPy gradient conductive membranes

The morphology of BC/PPy gradient conductive membranes was observed using field-emission scanning electron microscopy (FESEM, Sirion 200, Holland) at an accelerating voltage of 10 kV, following sputter coating with gold. Current flow through the membranes was measured by conductive atomic force microscopy (C-AFM, -0.1 V) using the current detection mode with the scanning size of 5 μm × 5 μm. The chemical composition of the membranes was analyzed by Fourier-transform infrared spectroscopy (FTIR) spectrometer (Vertex 70, Germany) in the spectral range of 500-4,000 cm^{-1}. Thermogravimetric analysis (TGA, Pyrisl, China) was performed to evaluate thermal properties, with measurements conducted under a nitrogen atmosphere at a heating rate of 10 °C/min from 25 °C to 800 °C. Elemental composition was identified by X-ray photoelectron spectroscopy (XPS) spectrum (AXIS-ULTRA DLD-600W, Shimadzu) and elemental analyzer (EA, Vario Micro cube, Elementar). Surface resistivity across different membrane segments was measured using a four-point probe resistivity meter. Mechanical properties were assessed using an Instron universal testing machine (UTM6503, SUNS Industrial Testing System Co., Ltd., China) at a stretching speed of 1 mm/min at 25 °C and 50% relative humidity. Young's modulus was determined from

the slope at low strain values, and the maximum tensile strength corresponded to the maximum stress at sample breakage. Contact angle (CA) measurements were performed by a drop-shape analyzer (DSA 100, Krüss). For each measurement, 10 μL of deionized water was dispensed onto different positions on the membrane surface, and the average contact angle was reported.

Biocompatibility evaluation and cell morphology observation

MTT assay and hemocompatibility

The cytotoxicity of BC/PPy gradient conductive membranes was evaluated using the MTT assay. NIH3T3 cells were cultured in DMEM medium supplemented with 1% P/S and 10% FBS at 37 °C with 5% CO_2. PC12 cells, which are widely used in nerve regeneration research, were cultured in RPMI 1640 medium supplemented with 5% horse serum, 5% FBS, and 1% P/S under the same conditions. Prior to cell seeding, the sterilized samples were pre-incubated in serum-free culture medium for 12 h. Then, cells were seeded onto the membranes at a density of 8×10^3 cells/well in 96-well plates. After 1, 3, and 5 days of culture, the culture medium was replaced with fresh medium containing 0.5 mg/mL MTT, and the cells were incubated at 37 °C for another 4 h. Then, 300 μL of DMSO was added and incubated for 10 minutes to dissolve the formazan crystals. The absorbance was measured at 490 nm using a microplate reader. The hemocompatibility of the membranes was assessed using a hemolytic activity assay as previously reported[29]. Initially, the materials were cut to fit into a 24-well plate and placed in each well. Then, 1 mL of 0.9% NaCl solution was added to each well, and the samples were pre-treated at 37 °C for 24 hours. After pre-treatment, the sample was transferred to test tubes, with 0.9 mL of physiological saline and 0.1 mL of diluted sheep whole blood added to each tube (V_whole blood: V_physiological saline = 1:1.25). After thorough mixing, the tubes were incubated at 37 °C for 1 h, followed by centrifugation at 1,000 rpm for 5 min. The supernatant was collected, and its absorbance was measured at 545 nm using a multi-functional microplate reader. Physiological saline was used as the negative control, and distilled water served as the positive control. Three parallel samples were used for each group.

The hemolysis rate of the samples was calculated using the following Equation 1[11]:

$$HR(\%) = [(OD_S - OD_N) / (OD_P - OD_N)] \times 100 \quad (1)$$

where OD_S, OD_N, and OD_P represented the optical density values of the sample, negative control, and positive control, respectively. This test provided insights into the hemocompatibility of the materials by evaluating their impact on red blood cell integrity.

Live/dead staining and cytoskeleton staining

The morphology of cells on the membranes was observed by confocal laser scanning microscopy (CLSM, Olympus FV1000, Japan) after 5 days of culture. For the live/dead staining, NIH3T3 and PC12 cells seeded on the membranes were stained using Calcein-AM (2 μM) and PI (4 μM) for 15 min at 37 °C, and then observed and imaged by CLSM. For the cytoskeleton staining, PC12 cells on membranes were first fixed with 4% paraformaldehyde for 30 min and then permeabilized with 0.1% Triton X-100 (v/v) for 5 min. Subsequently, the cells were co-stained with FITC-conjugated phalloidin and DAPI for 30 min prior to CLSM observation. ImageJ software was employed for statistical analysis and calculation of cell orientation angles. An angle of 0° indicates perfect alignment (parallel to the fiber alignment).

β3-tubulin staining

β3-Tubulin is considered an early neuronal differentiation marker and used for staining of neurites[30]. For the β3-tubulin staining, PC12 cells on the membranes were first fixed with 4% paraformaldehyde for 30 min,

permeabilized with 0.1% Triton X-100 (v/v) for 5 min and blocked with 2% BSA for 1 h. The cells were then incubated with β3-tubulin primary antibody at 4 °C for 12 h, followed with co-staining of rhodamine-conjugated goat anti-mouse IgG (H+L) and DAPI for 1 h at room temperature prior to CLSM observation.

Electrical stimulation of cells on the membranes

The homemade electrotaxis chamber was built on the culture dish as previously reported[11]. After one day of PC12 cells cultured on the membranes, the medium was replaced with differentiation medium containing 10% FBS and 50 ng/mL NGF for another 12 h. The samples were then placed in the electrotaxis chamber. A constant EF magnitude of 50 mV/mm was applied for 1 hour per day over two consecutive days. Finally, the cells were cultured for an additional 12 hours before staining.

Statistical analysis

Each experiment was performed in triplicate. Error bars represent standard deviation (SD). Comparisons between two groups were carried out by the Student's t-test, and differences were considered statistically significant at $^{*}P < 0.05$, $^{**}P < 0.01$, and $^{***}P < 0.001$.

RESULT AND DISCUSSION

Preparation and screening of BC/PPy gradient conductive membranes

To fabricate and identify the most suitable PPy gradient deposition on the membranes, three types of BC/PPy gradient conductive membranes were prepared with extraction rates of 10, 20, and 30 mL/min, respectively. The PPy gradient was formed by varying the deposition duration along the membrane. For characterization, each membrane was divided into three segments (upper, middle, and lower), with the lower segment having the longest deposition time. The surface morphology and elemental analysis confirmed the successful loading of PPy gradient onto all three membranes [Supplementary Figures 1 and 2]. The surface resistance and surface current measurements [Supplementary Figures 3 and 4] indicated that the surface conductivity of BC/PPy gradient conductive membranes increased from the upper to lower segments. The cell activity of NIH3T3 and PC12 cells on the 20-BC/PPy gradient conductive membranes was higher than that of the other groups [Supplementary Figure 3]. Therefore, 20-BC/PPy gradient conductive membranes, which demonstrated favorable biocompatibility and excellent gradient surface resistance characteristics, were selected for subsequent experiments unless otherwise specified.

Characterization of BC/PPy gradient conductive membranes

Morphological characterization

The surface morphology of upper, middle, and lower segments of the non-stretched and stretched BC/PPy gradient conductive membranes is shown in Figure 2. PPy nanoparticles with diameters of approximately 100 nm were successfully deposited onto the surface of BC nanofibers, exhibiting an increasing concentration gradient distribution from the upper to lower segments [Figure 2A-F]. The membrane color became darker with increasing PPy deposition [Supplementary Figure 5]. Specifically, the fibers in the non-stretched BC/PPy gradient conductive membranes were randomly arranged [Figure 2A-C], whereas the stretched BC/PPy gradient conductive membranes exhibited clear fiber alignment along the stretching direction [Figure 2D and F]. The cross-sectional morphologies of the stretched BC/PPy gradient conductive membranes further revealed their internal oriented structure [Figure 2G and H]. The fiber alignment characteristics were consistent with our previous study[11]. Moreover, PPy tended to polymerize along the fiber alignment of the stretched membranes, suggesting that the aligned BC nanofibers effectively guided PPy deposition. This may be attributed to the deeper grooves in the stretched membranes compared to the non-stretched ones [Figure 3], which facilitated the formation of aligned and continuous conductive fiber networks for electron transfer. Overall, the stretched BC/PPy gradient conductive membranes, featuring highly aligned nanofibers and a gradient conductive PPy structure, offer suitable topographical and electrical

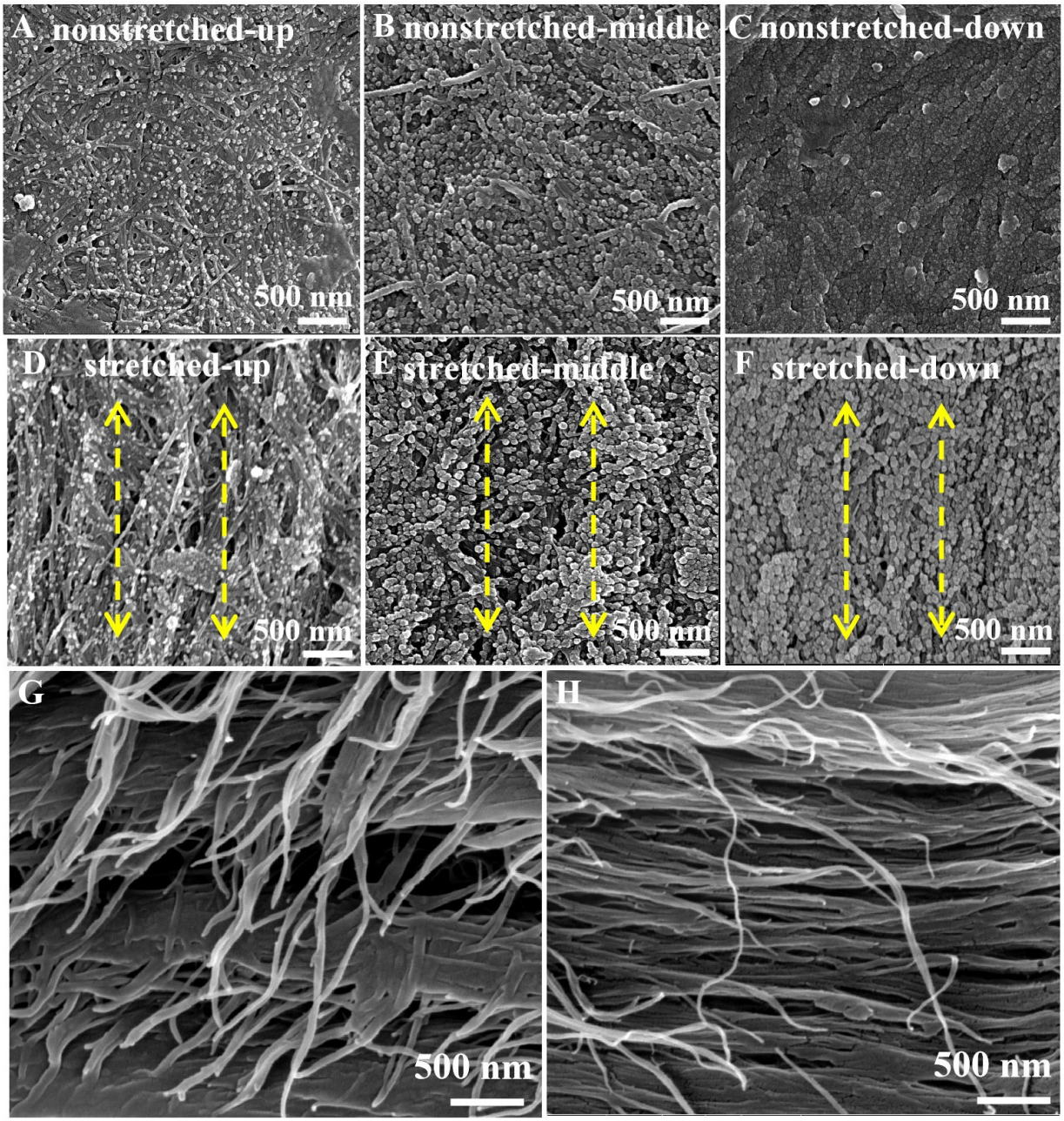

Figure 2. FESEM images of the BC/PPy gradient conductive membranes: (A-C) non-stretched membranes (upper, middle, and lower segments); (D-F) stretched membranes (upper, middle, and lower segments). Cross-sectional images of the stretched lower segment taken perpendicular to the stretching direction (G) and parallel to the stretching direction (H). Scale bar: 500 nm. FESEM: Field-emission scanning electron microscopy; BC: bacterial cellulose; PPy: polypyrrole.

guidance for further investigations into nerve cell behavior.

C-AFM

In view of the importance of surface topography and conductivity variations of biomaterials for the adhesion, proliferation, and differentiation of nerve cells[31], C-AFM[32,33] was performed, and the results are presented in Figure 3. On all BC/PPy gradient conductive membranes, the surface current increased with the rising concentration gradient of PPy from the upper to lower segments [Figure 3A-C and G-I], indicating improved electron transfer efficiency and conductivity after PPy incorporation[34]. The surface current

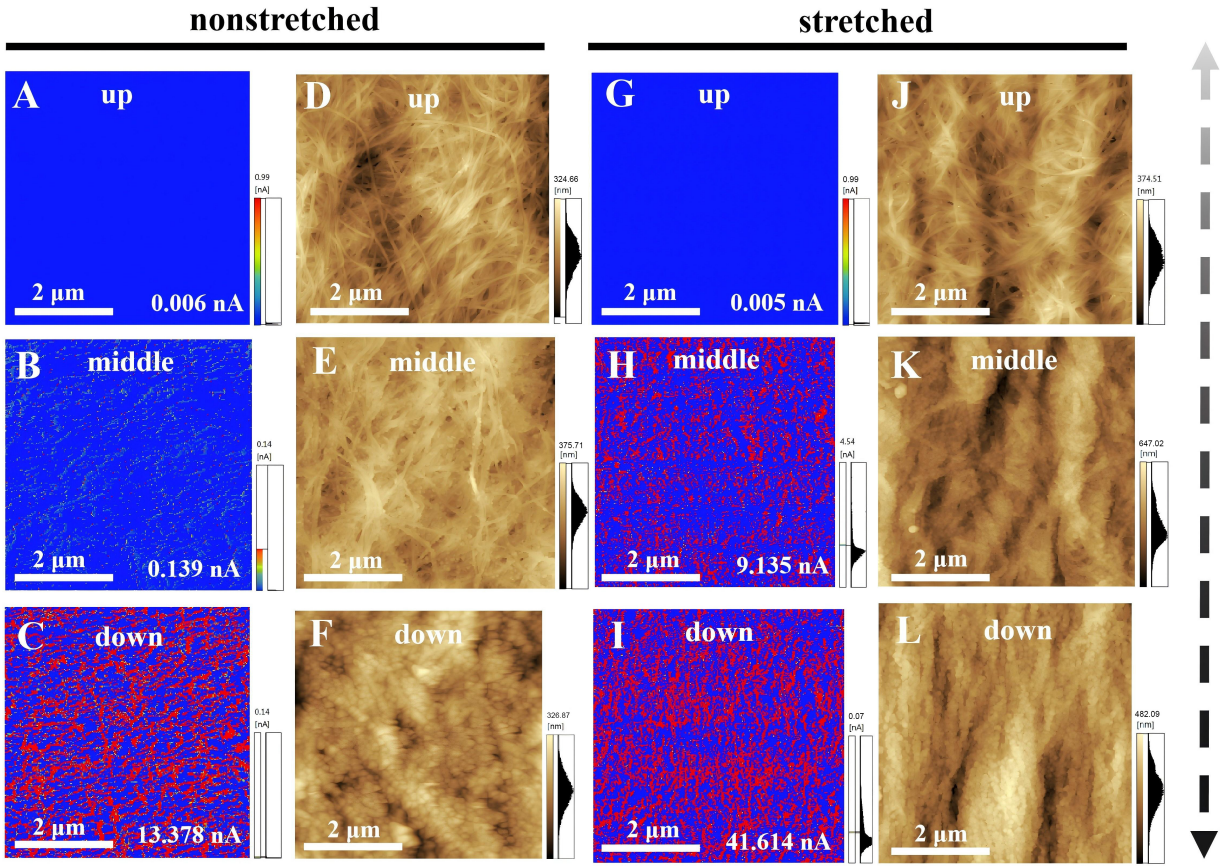

Figure 3. AFM images of non-stretched (A-F) and stretched (G-L) BC/PPy gradient conductive membranes. Current images are shown for non-stretched (A-C) and stretched (G-I) membranes, and height images for non-stretched (D-F) and stretched (J-L) membranes. Scan size: 5 μm × 5 μm. AFM: Atomic force microscopy; BC: bacterial cellulose; PPy: polypyrrole.

density on the upper, middle, and lower segments of the non-stretched BC/PPy gradient conductive membranes were 0.006, 0.139, and 13.378 nA, respectively [Figure 3A-C]. In comparison, the stretched membranes exhibited higher surface currents on the corresponding segments, with values of 0.005, 9.135, and 41.614 nA, respectively [Figure 3G-I]. Notably, the stretched BC/PPy gradient conductive membranes displayed an aligned surface current distribution along the fiber orientation, with the lower segment showing the maximum surface current (Figure 3I, 41.614 nA) and regular nanogroove depth (Figure 3L, 482.09 nm). In contrast, the non-stretched membranes exhibited randomly distributed surface currents and shallower nanogrooves. This difference may be attributed to the stretching and hot-pressing processes, which reduced the specific volume between nanofibers, thereby increasing nanogroove depth and promoting aligned PPy deposition for efficient current flow. Overall, the highly aligned stretched BC/PPy gradient conductive membranes exhibit gradient surface current distribution and enhanced current flow along the fiber alignment, making them promising candidates for guiding cell behavior via topographical and gradient cues in peripheral nerve regeneration.

Fourier transform infrared spectra and thermogravimetric analysis

FTIR was performed on BC and stretched BC/PPy gradient conductive membranes to evaluate the effect of *in-situ* PPy polymerization on the chemical structure [Figure 4A]. The spectrum of BC reveals that bands at 3,344, 2,896, 1,646, and 1,051 cm^{-1} were attributed to the stretching vibrations of O-H, C-H, and deformation vibrations of O-H, C-O, respectively. For the BC/PPy gradient conductive membranes, new characteristic peaks at 1,543 and 1,453 cm^{-1}, corresponding to the stretching vibrations of C=C and C=N in pyrrole,

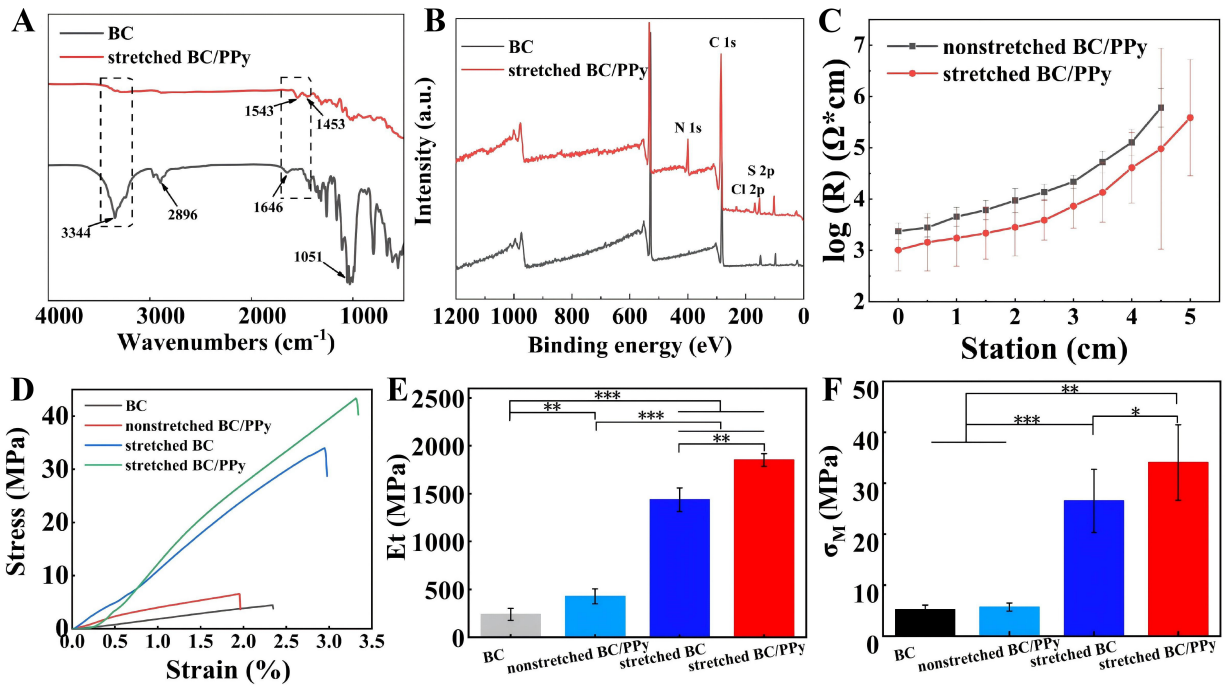

Figure 4. Characterizations of BC/PPy conductive gradient membranes. ATR-FTIR (A) and XPS (B) spectra of BC and stretched BC/PPy conductive gradient membranes; (C) The log (R) values of non-stretched and stretched BC/PPy conductive gradient membranes. (D-F) Stress-strain, Young's modulus and tensile strength curves of BC, non-stretched BC/PPy,stretched BC, and stretched BC/PPy conductive gradient membranes. $n = 3$, $^{*}P < 0.05$, $^{**}P < 0.01$, $^{***}P < 0.001$. Error bars represent SD. BC: Bacterial cellulose; PPy: polypyrrole; ATR: attenuated total reflectance; FTIR: Fourier-transform infrared spectroscopy; XPS: X-ray photoelectron spectroscopy; SD: standard deviation.

respectively, confirming successful PPy polymerization on the BC membranes[34,35]. Compared with pure BC, the BC/PPy gradient conductive membranes exhibited a gradual reduction in the absorption peak at 3,344 cm^{-1}, along with a slight shift to 3,340 cm^{-1}. This change is attributed to hydrogen-bonding interactions between BC and PPy, which altered the original O-H connections on BC and resulted in a redshift of the infrared stretching vibration peak. Simultaneously, increased PPy deposition on the gradient-conductive membranes fibers led to a decrease in the intensity of the O-H stretching vibration peak. In addition, Thermogravimetric analysis TGA was conducted to evaluate the thermal stability of non-stretched and stretched BC/PPy gradient conductive membranes at different segments [Supplementary Figure 6]. Three decomposition stages were observed for all the gradient conductive membranes. Notably, the thermal stability of BC/PPy gradient-conductive membranes improved with increasing PPy content. Furthermore, the stretched membranes exhibited superior thermal stability compared to non-stretched membranes, which may be attributed to the denser structure of the aligned BC/PPy fibers. This aligned structure acts as a barrier to BC molecular chains, further enhancing thermal stability for tissue engineering applications[11].

X-ray photoelectron spectroscopy analysis

XPS was used on different segments of non-stretched and stretched BC/PPy gradient conductive membranes. Compared with BC, the lower segment of the aligned BC/PPy gradient conductive membranes exhibited a new characteristic N peak at 398 eV, confirming successful PPy loading [Figure 4B]. The newly emerged S peak was attributed to the incorporation of p-TSA during PPy synthesis. Further quantitative analysis of N content in the different membranes is shown in Supplementary Table 1. For the non-stretched BC/PPy gradient conductive membranes, the N content in the upper, middle, and lower segments increased sequentially to 3.57%, 5.32%, and 9.37%, respectively. A similar trend was observed for the stretched membranes, with N contents of 3.9%, 8.3%, and 9.6% in the upper, middle, and lower segments, respectively,

indicating effective PPy gradient deposition from the upper to lower segments. Notably, the stretched membranes exhibited slightly higher N content in the corresponding segments compared with the non-stretched membranes under the same reaction time. This can be attributed to the more aligned and tightly packed BC nanofibers, which provide a topographical structure conducive to increased *in-situ* PPy deposition. These results are consistent with the FESEM and C-AFM analyses, collectively highlighting the effectiveness of PPy gradient deposition and the influence of aligned nanofibers on the structural and compositional characteristics of the BC/PPy gradient conductive membranes.

Surface resistance analysis and hydrophilicity analysis

The surface resistance of the non-stretched and stretched BC/PPy gradient conductive membranes was evaluated using a surface resistance meter [Figure 4C]. A gradual increase in surface resistance from the lower to the upper segments was observed across all BC/PPy gradient conductive membranes [Supplementary Figure 3]. Notably, the stretched BC/PPy gradient conductive membranes exhibited lower surface resistance than their non-stretched counterparts at the same segments. This can be attributed to the greater amount of PPy deposited on the aligned nanofibers due to their larger deposition area, which facilitated the formation of continuous and oriented conductive pathways, thereby enhancing electron transport efficiency. These surface resistance results are consistent with the C-AFM findings, further confirming the successful fabrication of BC/PPy gradient conductive membranes for guiding cellular activities. In addition, surface hydrophilicity analysis revealed a gradient change in surface hydrophilicity across the BC/PPy gradient conductive membranes [Supplementary Table 2]. This trend can be explained by the gradient increase in PPy deposition on the BC nanofibers from the upper to lower segments, which led to a gradient reduction in active hydrophilic groups (-OH) on the nanofibers. Such tunable surface properties may facilitate cell-material interactions in specific tissue engineering applications

Mechanical property

Mechanical properties are critical parameters for evaluating tissue-engineering scaffolds derived from biomaterials[36]. The mechanical properties of the non-stretched and stretched BC/PPy gradient conductive membranes are presented in Figure 4D-F. The pure BC membrane exhibited a tensile strength of 5.2 MPa and a Young's modulus of 238.6 MPa, whereas the stretched BC/PPy gradient conductive membranes achieved a tensile strength of 34.1 MPa ($P < 0.01$) and a Young's modulus of 1,849.9 MPa ($P < 0.001$). Previous studies have also reported that tensile strength and Young's modulus increase with PPy deposition and nanofiber alignment[11,37]. In the present study, the enhanced mechanical properties of the stretched BC/PPy gradient conductive membranes can be attributed to two factors. First, the aligned nanofibers are densely packed and form stronger hydrogen bonds. When subjected to tensile forces along the alignment direction, the inherently stronger fibers in the oriented membranes can withstand greater external loads. In contrast, in the non-stretched BC/PPy gradient conductive membranes, only a few fibers align with the direction of the applied force, leading to simultaneous rupture of most fibers, as previously reported[11]. Second, PPy deposition on the aligned BC fibers is denser and more continuous, reinforcing hydrogen-bonding interactions both between PPy and BC and among BC fibers. In conclusion, the combined effects of PPy deposition and nanofiber alignment synergistically improved the mechanical properties of the BC/PPy gradient conductive membranes, supporting their potential application in nerve regeneration.

In vitro biocompatibility evaluation and cell morphology

Biocompatibility is a fundamental requirement for biomaterials in tissue engineering applications[38]. The hemolysis ratio (HR) was employed to evaluate the blood compatibility of non-stretched and stretched BC/PPy gradient conductive membranes [Figure 5A]. For the non-stretched gradient-conductive membranes, the HR values of the upper, middle, and lower segments were 1.38%, 0.28%, and 0.28%, respectively, while the stretched membranes exhibited HR values of 0.87%, 0.04%, and 0.40% at the

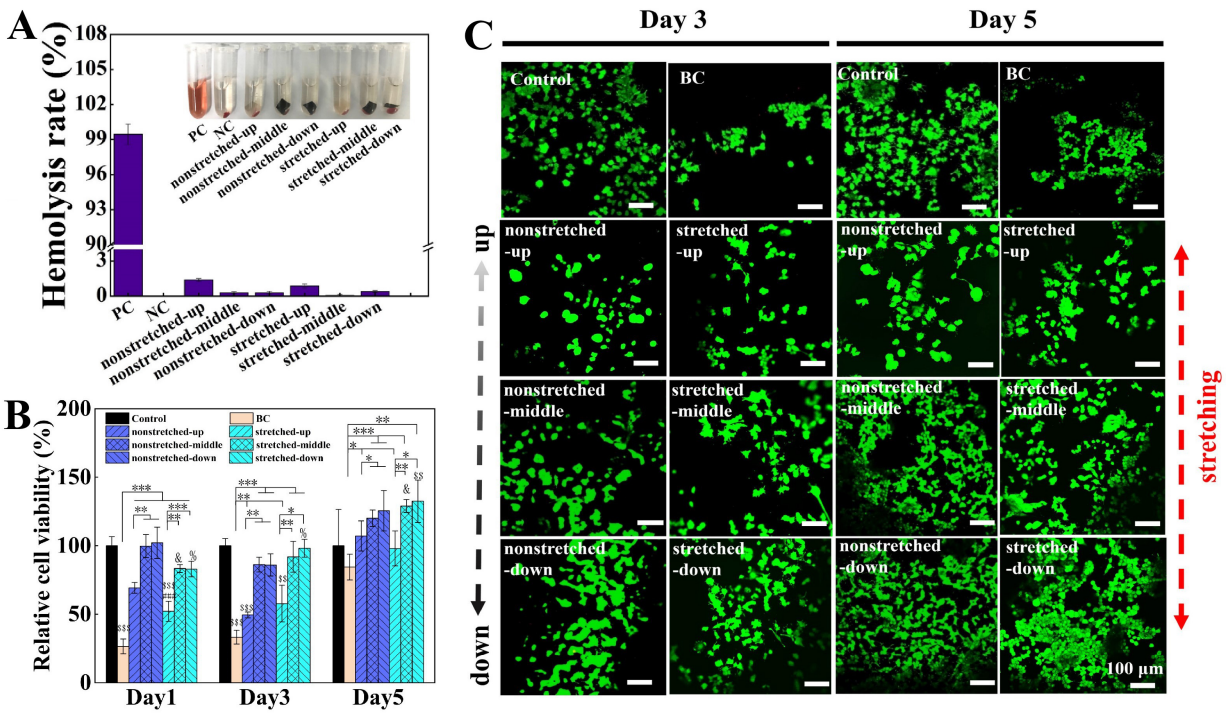

Figure 5. Biocompatibility of BC/PPy conductive gradient membranes and cell morphology observations. (A) Hemolysis test for non-stretched and stretched BC/PPy conductive gradient membranes. PC: positive control (distilled water); NC: negative control (normal saline), $n = 3$; (B and C) MTT assay and Live/Dead staining images of PC12 cells cultured on Control (petri dish), BC, non-stretched and stretched BC/PPy conductive gradient membranes. $n = 3$, $^{*}P < 0.05$, $^{**}P < 0.01$, $^{***}P < 0.001$, $^{\#\#}P < 0.01$, # when compared with the non-stretched upper segment under the same conditions. $^{\&}P < 0.05$, & when compared with the non-stretched middle segment under the same condition. $^{\%}P < 0.05$, % when compared with the non-stretched lower segment under the same condition. $^{\$\$}P < 0.01$, $^{\$\$\$}P < 0.001$, $ when compared with control group under the same condition. Scale bars are 100 μm. Error bars represent standard deviation (SD). BC: Bacterial cellulose; PPy: polypyrrole; MTT: 3- (4,5-dimethylthiazol-2-yl)-2,5-diphenyltetrazolium bromide.

corresponding segments. These results indicate good hemocompatibility of the BC/PPy gradient conductive membranes, as a hemolysis ratio below 5% is considered acceptable for biomaterials[39].

The cytocompatibility of BC, non-stretched, and stretched BC/PPy gradient conductive membranes was assessed via MTT assays using PC12 and NIH3T3 cells [Figure 5B and Supplementary Figure 7]. Throughout the 1, 3, and 5-day culture periods, cell viability on all BC/PPy gradient conductive membranes was higher than that on pure BC membranes, indicating the non-cytotoxic nature of the BC/PPy membranes. Specifically, for the non-stretched gradient-conductive membranes, the relative cell viability of the middle and lower segments (120% and 126%, respectively) was significantly higher than that of the upper segment (107%, $P < 0.05$). A similar gradient in cell viability was observed for the stretched BC/PPy gradient conductive membranes, with relative cell viability values of 98% (upper), 129% (middle, $P < 0.01$), and 132% (lower, $P < 0.05$). Notably, the lower segment of the stretched BC/PPy gradient conductive membranes exhibited the greatest promotion of cell proliferation, showing a 1.32-fold increase in cell viability compared with the control (culture dish, $P < 0.01$). Consistent results were obtained from the live/dead staining assay [Figure 5C]. From day 3 to day 5, a clear gradient in the proliferation of live cells (green) was observed across all gradient conductive membranes from the upper to lower segments, indicating that PC12 cells could proliferate and grow normally on the BC/PPy gradient conductive membranes, particularly on the lower segment of the stretched membranes.

It is well established that PPy has excellent biocompatibility and can support cell proliferation[40]. In this study, the increasing concentration gradient of PPy on the aligned membranes contributed to the enhanced cell viability from the upper to lower segments. This phenomenon can be attributed to two factors. First, the

gradient PPy deposited on the stretched BC/PPy gradient conductive membranes was predominantly distributed along the fiber orientation [Figure 2D], which may facilitate more effective transmission of endogenous electrical signals between cells and fibers, thereby promoting cell proliferation[41]. Second, the deeper and oriented nanogrooves on the stretched BC/PPy gradient conductive nanofibers provide greater space for PPy deposition, offering more active functional groups and anchoring points for cell adhesion, growth, and proliferation[42]. Together, these results indicate that the stretched BC/PPy gradient conductive membranes promote gradient cell proliferation from the upper to lower segments, providing an effective strategy to couple topographical (fiber alignment) and gradient (PPy gradient) cues with subcellular responses.

Evaluation of cell differentiation on BC/PPy gradient conductive membranes

In the absence of EF

In the absence of an EF, PC12 cells cultured on the control dish, BC membranes, and the upper segment of non-stretched BC/PPy gradient conductive membranes exhibited a rounded morphology without protrusions. In contrast, cells on the middle and lower segments of the non-stretched BC/PPy membranes began to display protrusions (Figure 6 and 7A, -EF). Compared with the same segments of the non-stretched BC/PPy gradient conductive membranes, more cell protrusions and longer neurites were observed on the stretched BC/PPy membranes with neurites elongate along the fiber alignment. Significantly higher neurite-bearing cell population ($P < 0.01$) and neurites length ($P < 0.01$) on the lower segment are measured than that on the upper segment of BC/PPy gradient conductive membranes (Figure 7B and C, -EF). Moreover, both the neurite-bearing cell population ($P < 0.05$) and neurite length ($P < 0.001$) on the lower segment of the stretched membranes were significantly higher than those on the non-stretched counterparts (Figure 7B and C, -EF). These results indicate a gradient in cell differentiation from the upper to lower segments of the BC/PPy gradient conductive membranes, with the lower segment of the stretched membranes exhibiting the greatest effect. In addition, as shown in Figure S8, the stretched BC/PPy gradient conductive membranes promoted neurite elongation along the fiber alignment, particularly on the lower segment. This finding is consistent with previous reports showing oriented growth of PC12 cells and Schwann cells on patterned materials[12,43]. Another study demonstrated enhanced neurogenesis of PC12 cells on aligned conductive scaffolds[44]. In this study, the gradient and directional cell differentiation observed on the stretched BC/PPy gradient conductive membranes may be attributed to the gradient and aligned deposition of PPy, which can transmit gradient electrical signals to conductive cells such as PC12 cells, thereby influencing cellular signaling pathways and inducing directional cell differentiation.

In the presence of EF

To further investigate the synergistic effect of the BC/PPy gradient conductive membranes and EF on cell differentiation, PC12 cells cultured on the membranes were exposed to EF (Figure 6 and 7A, +EF). Notably, cells in the "+EF" groups exhibited typical neuronal differentiation morphology with well-formed neurites [Figure 6 and 7A]. The neurite-bearing cell population and neurite length measured on all segments of the BC/PPy gradient conductive membranes under EF were significantly higher than those without EF, except for the upper segment of the stretched membrane [Figure 7B and C]. Moreover, the lower segment of the stretched membranes in the presence of EF exhibited the highest neurite-bearing cell population (Figure 7B, 63.35%), which was 1.29-fold higher than that of the lower segment of the non-stretched membranes (49.03%, $P < 0.05$, +EF) and 2.04-fold higher than that of the upper segment of the stretched membranes (31.13%, $P < 0.05$, +EF). A similar trend was observed for neurite length, where the lower segment of the stretched membranes under EF (Figure 7C, 64.39 μm) exhibited a 1.45-fold increase compared with the lower segment of the non-stretched membranes (44.38 μm, $P < 0.001$, +EF) and a 1.82-fold increase compared with the upper segment of the stretched membranes (35.43 μm, $P < 0.001$, +EF).

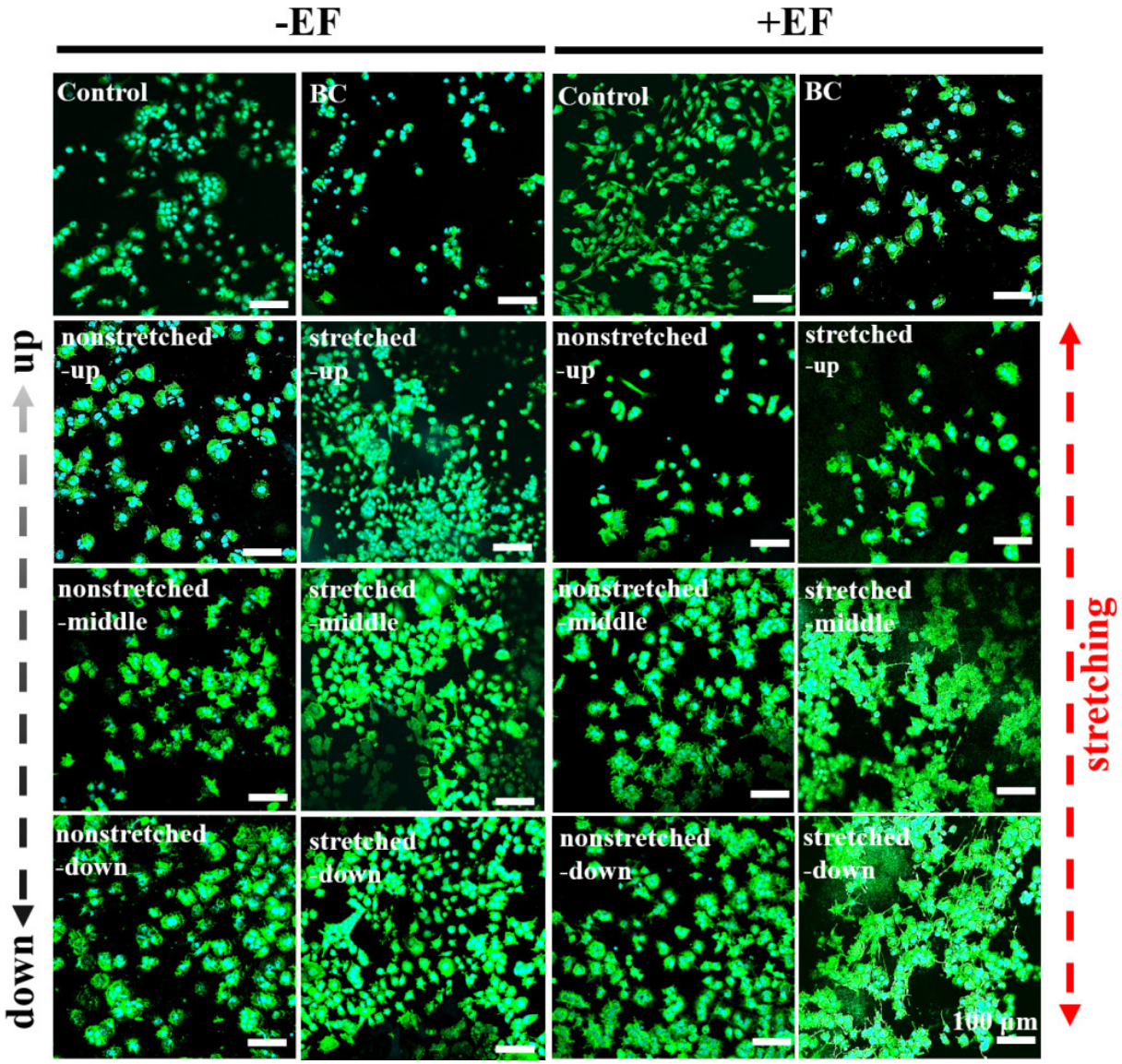

Figure 6. The synergistic effect of BC/PPy gradient conductive membranes and EF on PC12 cells. FITC/DAPI staining images of PC12 cells after culturing on Control (petri dish), BC, non-stretched and stretched BC/PPy gradient conductive membranes in the absence or presence of EF, respectively. Scale bars are 100 μm. EF: Electric field; BC: bacterial cellulose; PPy: polypyrrole; PC12: pheochromocytoma; FITC: Fluorescein isothiocyanate; DAPI: dihydrochloride.

In addition, Supplementary Figure 8 shows that EF did not significantly affect the direction of neurite extension. This finding suggests that, under our experimental conditions, topographical contact guidance from the aligned BC nanofibers dominates over electrotactic cues from the external EF in directing neurite polarity. This may be due to the following reasons. First, the strength of the applied EF (50 mV/mm) may be below the threshold required to induce directional migration or neurite turning in PC12 cells. Previous studies have shown significant threshold differences in the responses of different cell types to electric fields[45]. Second, the intermittent nature of EF application (1 h per day) may limit its directional influence. Continuous EF exposure is often required for sustained electrotaxis, whereas our protocol prioritized cell viability and mimicked clinically relevant intermittent stimulation. In contrast, the topographical cues are present constantly and provide persistent directional signals through cytoskeletal reorganization and focal adhesion alignment[7,44]. Thus, in our system, the aligned BC/PPy gradient membrane provides the directional template, while EF serves as a non-directional trophic factor that amplifies the extent of differentiation. This

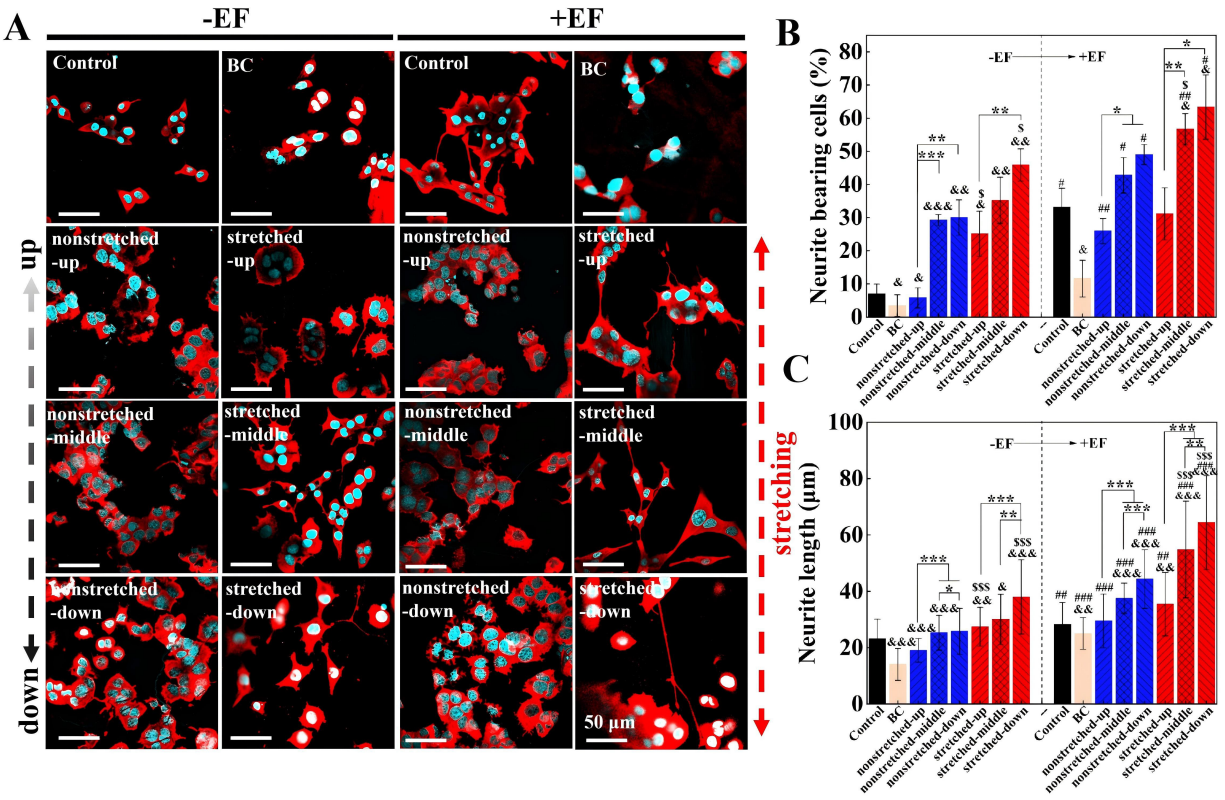

Figure 7. The synergistic effect of BC/PPy gradient conductive membranes and EF on differentiation of PC12 cells. (A) Immunofluorescence images of PC12 cells after culturing on Control (petri dish), BC, non-stretched and stretched BC/PPy gradient conductive membranes in the absence or presence of electrical stimulation, respectively. Scale bars are 50 μm; (B and C) Quantitative analysis of the neurite-bearing (B), neurite length (C) of PC12 cells after culturing on Control (petri dish), BC, non-stretched lower and stretched lower BC/PPy gradient conductive membranes in the absence or presence of electrical stimulation, respectively. $n = 3$, $^{*}P < 0.05$, $^{**}P < 0.01$, $^{***}P < 0.001$, $^{\&}P < 0.05$, $^{\&\&}P < 0.01$, $^{\&\&\&}P < 0.001$, & when compared with Control group under the same condition. $^{\#}P < 0.05$, $^{\#\#}P < 0.01$, $^{\#\#\#}P < 0.001$, # when compared with "-EF" groups under the same condition. $^{\$}P < 0.05$, $^{\$\$\$}P < 0.001$, $ when compared with non-stretched groups under the same condition. Error bars represent standard deviation (SD). BC: Bacterial cellulose; PPy: polypyrrole; EF: electric field; PC12: pheochromocytoma.

complementary synergy is highly favorable for nerve repair, as it ensures guided regeneration along the desired axis while maximizing neurite extension.

Collectively, the combination of stretched BC/PPy membranes with EF synergistically enhanced the neurite-bearing cell population and neurite length in a gradient manner from the upper to lower segments. Similar enhancements in cell differentiation have been reported by Tang *et al.*, who demonstrated that the combination of conductive PPy-coated aligned fibers with EF collectively promoted functional expression in PC12 cells, including elongation, gene expression, and protein expression[13]. Previous studies have suggested that a conductive microenvironment combined with EF facilitates the opening of voltage-gated calcium channels and calcium ion influx, thereby upregulating the expression of neurogenic genes and enhancing neurogenesis[46,47]. However, the combined influence of gradient-conductive and topographical guidance, together with EF, on cell differentiation has remained unexplored.

The synergistic effect of the aligned BC/PPy gradient conductive membranes combined with electrical stimulation can be attributed to three main factors. First, regarding the PPy gradient guidance, the conjugated π-electron clouds along the aligned PPy gradient chains form delocalized electron systems, enabling continuous and gradient charge transmission. This effectively promotes intracellular signal transduction between cells and the material, thereby enhancing gradient neuronal differentiation from the

upper to lower segments of the membranes. Second, concerning topographical guidance, the aligned BC nanofibers serve as a core structural component, resembling nerve bundles composed of numerous aligned cell-matrix assemblies[48]. Moreover, PPy possesses favorable biocompatibility and supports the adhesion, growth, and differentiation of neural cells[49]. Consequently, the oriented deposition of PPy along the aligned BC nanofibers can activate relevant cellular signaling pathways, converting topographical cues into mechanical signals and subsequently inducing cell differentiation. Third, with respect to the application of EF, studies have demonstrated its important role in altering the distribution of extracellular matrix molecules and enhancing protein adsorption, thereby promoting neural axon elongation. In the present study, electrical stimulation concurrently induces the transfer of delocalized π electrons along the oriented PPy chains, facilitating the transport of bioactive molecules or growth factors and contributing to the conversion of topographical signals into mechanical signals. Ultimately, these combined effects synergistically achieve gradient differentiation of PC12 cells on the aligned BC/PPy gradient conductive membranes.

Overall, the stretched BC/PPy gradient conductive membranes effectively enhance directional neurite outgrowth and neurite length in a gradient manner from the upper to lower segments. Notably, under electrical stimulation, cells exhibit the most pronounced differentiation along the fiber alignment on the lower segment of the stretched membranes. Wang *et al.* developed a composite nerve conduit consisting of aligned PLCL nanofiber conduits and aligned GelMA hydrogel, which effectively promoted axonal regeneration, remyelination, and angiogenesis[50], while Jin *et al.* developed a conductive fibrous hydrogel bandage that achieved effective nerve regeneration and functional recovery[51]. Our results are consistent with these recent findings and are the first to report synergistically enhanced gradient cell differentiation achieved by combining stretched BC/PPy gradient conductive membranes with EF stimulation, highlighting the potential of integrating these cues for peripheral nerve regeneration.

CONCLUSION

In summary, a highly aligned BC/PPy gradient-conductive membrane was successfully fabricated via quantitative stretching and hot pressing of BC, followed by a kinetically controlled in situ polymerization to introduce a gradient distribution of PPy along the nanofibers. The resulting membrane exhibited well-aligned nanofibers with a gradient PPy deposition along the fiber alignment, demonstrating good mechanical strength, thermal stability, and a gradient in surface current. In vitro biological evaluations revealed that the aligned BC/PPy gradient-conductive membrane possessed excellent cytocompatibility and hemocompatibility, and effectively promoted gradient proliferation and differentiation of PC12 cells. Furthermore, upon application of an EF, directional gradient cell differentiation on the aligned BC/PPy gradient conductive membrane was significantly enhanced, with the maximum neurite length (64.39 μm) and neurite-bearing cell population (63.35%) observed on the lower segment, compared with the non-stretched BC/PPy gradient conductive membrane under EF and the stretched BC/PPy membrane without EF. These results suggest a synergistic effect between the aligned BC membrane and EF in promoting nerve regeneration. Taken together, the findings support our hypothesis that the aligned BC/PPy gradient-conductive membrane, combined with EF, represents a promising strategy for enhancing directional cell differentiation in accelerated peripheral nerve regeneration.

DECLARATIONS

Acknowledgements

The authors acknowledge the Analytical and Testing Centre at HUST for performing characterization of various samples.

Authors' contributions

Investigation: Wang, L.; Wang, H.
Methodology: Wang, L.; Wang, H.
Writing: Wang, L.; Qi, F.

Review: Qi, F.; Hu, S.
Data: Wang, H.; Li, S.
Visualization: Hu, S.
Conceptualization: Shi, Z.
Supervision: Shi, Z.; Yang, G.
Project administration: Yang, G.

Availability of data and materials

The original contributions presented in this study are included in the article/Supplementary Materials. Further inquiries can be directed to the corresponding authors.

AI and AI-assisted tools statement

Not applicable.

Financial support and sponsorship

This work was supported by the National Key Research and Development Program of China (Grant No. 2025YFE0120100), the National Natural Science Foundation of China (Grant No. 52373235 and 52573322), State Key Laboratory of Advanced Papermaking and Paper-based Materials (Project Number 202509), Hubei Provincial Health Special Project (2025CDB024).

Conflicts of interest

Yang, G. is an Associate Editor of *Iontronics*. Yang, G. and Shi, Z. serve as Guest Editors of the Special Issue "Frontiers in Bioelectronic Interface and Electrical Stimulation Therapy" in *Iontronics*. They were not involved in any aspect of the editorial processing of this manuscript, including reviewer selection, manuscript handling, or decision-making. The other authors declare no conflicts of interest.

Ethical approval and consent to participate

Not applicable.

Consent for publication

Not applicable.

Supplementary Materials

Supplementary Materials

REFERENCES

1. Luo, Y.; Li, J.; Li, B.; Xia, Y.; Wang, H.; Fu, C. Physical cues of matrices reeducate nerve cells. *Front. Cell. Dev. Biol.* **2021**, *9*, 731170. DOI PubMed PMC
2. Wang, J.; Zhu, Y.; Wang, Y.; et al. A novel tissue engineered nerve graft constructed with autologous vein and nerve microtissue repairs a long-segment sciatic nerve defect. *Neural. Regen. Res.* **2021**, *16*, 143. DOI
3. Heinzel, J. C.; Quyen Nguyen, M.; Kefalianakis, L.; et al. A systematic review and meta-analysis of studies comparing muscle-in-vein conduits with autologous nerve grafts for nerve reconstruction. *Sci. Rep.* **2021**, *11*, 11691. DOI PubMed PMC
4. Kehoe, S.; Zhang, X.; Boyd, D. FDA approved guidance conduits and wraps for peripheral nerve injury: A review of materials and efficacy. *Injury* **2012**, *43*, 553-72. DOI
5. Grinsell, D.; Keating, C. P. Peripheral nerve reconstruction after injury: a review of clinical and experimental therapies. *Biomed. Res. Int.* **2014**, *2014*, 1-13. DOI PubMed PMC
6. Javeed, S.; Faraji, A. H.; Dy, C.; Ray, W. Z.; Macewan, M. R. Application of electrical stimulation for peripheral nerve regeneration: Stimulation parameters and future horizons. *Interdiscip. Neurosur.* **2021**, *24*, 101117. DOI
7. Zhang, K.; Zheng, H.; Liang, S.; Gao, C. Aligned PLLA nanofibrous scaffolds coated with graphene oxide for promoting neural cell growth. *Acta. Biomater.* **2016**, *37*, 131-42. DOI

8. Manan, S.; Ullah, M. W.; Ul-Islam, M.; Shi, Z.; Gauthier, M.; Yang, G. Bacterial cellulose: Molecular regulation of biosynthesis, supramolecular assembly, and tailored structural and functional properties. *Prog. Mater. Sci.* **2022**, *129*, 100972. DOI
9. Ren, Y.; Zhang, S.; Mi, R.; et al. Enhanced differentiation of human neural crest stem cells towards the Schwann cell lineage by aligned electrospun fiber matrix. *Acta. Biomater.* **2013**, *9*, 7727-36. DOI
10. Wang, L.; Adhikari, M.; Li, L.; et al. Electrically stimulated Acetobacter xylinum for the production of aligned 3D microstructured bacterial cellulose. *Cellulose* **2023**, *30*, 9973-88. DOI
11. Wang, L.; Mao, L.; Qi, F.; et al. Synergistic effect of highly aligned bacterial cellulose/gelatin membranes and electrical stimulation on directional cell migration for accelerated wound healing. *Chem. Eng. J.* **2021**, *424*, 130563. DOI
12. Huang, Z.; Sun, M.; Li, Y.; Guo, Z.; Li, H. Reduced graphene oxide-coated electrospun fibre: effect of orientation, coverage and electrical stimulation on Schwann cells behavior. *J. Mater. Chem. B.* **2021**, *9*, 2656-65. DOI
13. Tang, J.; Wu, C.; Chen, S.; et al. Combining electrospinning and electrospraying to prepare a biomimetic neural scaffold with synergistic cues of topography and electrotransduction. *ACS. Appl. Bio. Mater.* **2020**, *3*, 5148-59. DOI
14. Sadeghi, A.; Moztarzadeh, F.; Aghazadeh Mohandesi, J. Investigating the effect of chitosan on hydrophilicity and bioactivity of conductive electrospun composite scaffold for neural tissue engineering. *Int. J. Biol. Macromol.* **2019**, *121*, 625-32. DOI
15. Liu, R.; Huang, X.; Wang, X.; et al. Electrical stimulation mediated the neurite outgrowth of PC-12 cells on the conductive polylactic acid/reduced graphene oxide/polypyrrole composite nanofibers. *Appl. Surf. Sci.* **2021**, *560*, 149965. DOI
16. Sun, Y.; Quan, Q.; Meng, H.; et al. Enhanced neurite outgrowth on a multiblock conductive nerve scaffold with self-powered electrical stimulation. *Adv. Healthc. Mater.* **2019**, *8*, 1900127. DOI
17. Chen, S.; Mccarthy, A.; John, J. V.; Su, Y.; Xie, J. Converting 2D nanofiber membranes to 3D hierarchical assemblies with structural and compositional gradients regulates cell behavior. *Adv. Mater.* **2020**, *32*, 2003754. DOI PubMed PMC
18. Moore, K.; Macsween, M.; Shoichet, M. Immobilized concentration gradients of neurotrophic factors guide neurite outgrowth of primary neurons in macroporous scaffolds. *Tissue. Eng.* **2006**, *12*, 267-78. DOI
19. Cai, Y.; Huang, Q.; Wang, P.; et al. Conductive hydrogel conduits with growth factor gradients for peripheral nerve repair in diabetics with non-suture tape. *Adv. Healthc. Mater.* **2022**, *11*, 2200755. DOI
20. Zhang, D.; Li, Z.; Shi, H.; et al. Micropatterns and peptide gradient on the inner surface of a guidance conduit synergistically promotes nerve regeneration *in vivo*. *Bioact. Mater.* **2022**, *9*, 134-46. DOI
21. Tang, S.; Zhu, J.; Xu, Y.; Xiang, A. P.; Jiang, M. H.; Quan, D. The effects of gradients of nerve growth factor immobilized PCLA scaffolds on neurite outgrowth *in vitro* and peripheral nerve regeneration in rats. *Biomaterials* **2013**, *34*, 7086-96. DOI
22. Zonderland, J.; Rezzola, S.; Wieringa, P.; Moroni, L. Fiber diameter, porosity and functional group gradients in electrospun scaffolds. *Biomed. Mater.* **2020**, *15*, 045020. DOI
23. Xue, T.; Yang, Y.; Yu, D.; et al. 3D printed integrated gradient-conductive MXene/CNT/polyimide aerogel frames for electromagnetic interference shielding with ultra-low reflection. *Nano-Micro. Lett.* **2023**, *15*, 45. DOI PubMed PMC
24. Shan, Y.; Feng, H.; Li, Z. Electrical stimulation for nervous system injury: Research progress and prospects. *Acta. Phys. Chim. Sin.* **2020**, 2005038. DOI
25. Costello, M. C.; Errante, E. L.; Smartz, T.; Ray, W. Z.; Levi, A. D.; Burks, S. S. Clinical applications of electrical stimulation for peripheral nerve injury: a systematic review. *Front. Neurosci.* **2023**, *17*, 1162851. DOI PubMed PMC
26. Zha, F.; Chen, W.; Hao, L.; et al. Electrospun cellulose-based conductive polymer nanofibrous mats: composite scaffolds and their influence on cell behavior with electrical stimulation for nerve tissue engineering. *Soft. Matter.* **2020**, *16*, 6591-8. DOI
27. Fan, Z.; Yu, W.; Wen, X.; Ding, X.; Li, X. Aligned conductive magnetic nanofibers with directional magnetic field stimulation promotes peripheral nerve regeneration. *Adv. Sci.* **2025**, *12*, e01665. DOI PubMed PMC
28. Yao, S.; Yang, Y.; Li, C.; et al. Axon-like aligned conductive CNT/GelMA hydrogel fibers combined with electrical stimulation for spinal cord injury recovery. *Bioact. Mater.* **2024**, *35*, 534-48. DOI PubMed PMC
29. Li, X.; Ji, X.; Chen, K.; et al. Development of finasteride/PHBV@polyvinyl alcohol/chitosan reservoir-type microspheres as a potential embolic agent: from *in vitro* evaluation to animal study. *Biomater. Sci.* **2020**, *8*, 2797-813. DOI
30. Prasannan, P.; Siney, E.; Chatterjee, S.; et al. A 3D-induced pluripotent stem cell-derived human neural culture model to study certain molecular and biochemical aspects of Alzheimer's disease. *In. vitro. models.* **2022**, *1*, 447-62. DOI PubMed PMC
31. Liu, F.; Xu, J.; Wu, L.; et al. The influence of the surface topographical cues of biomaterials on nerve cells in peripheral nerve regeneration: a review. *Stem. Cells. Int.* **2021**, *2021*, 1-13. DOI PubMed PMC
32. Mikulik, D.; Ricci, M.; Tutuncuoglu, G.; et al. Conductive-probe atomic force microscopy as a characterization tool for nanowire-based solar cells. *Nano. Energy.* **2017**, *41*, 566-72. DOI
33. Pathak, C. S.; Chang, B.; Song, S. Review on scanning probe microscopy analysis for perovskite materials and solar cells. *Dyes. Pigm.* **2023**, *218*, 111469. DOI

34. Xiong, F.; Wei, S.; Wu, S.; et al. Aligned electroactive electrospun fibrous scaffolds for peripheral nerve regeneration. *ACS. Appl. Mater. Interfaces.* **2023**, *15*, 41385-402. DOI
35. Thakur, A. V.; Lokhande, B. J. Study of RuO_2 incorporated PPy hybrid flexible electrodes prepared by soaking and drying technique: a novel approach. *Appl. Phys. A.* **2021**, *127*, 910. DOI
36. Dado, D.; Levenberg, S. Cell-scaffold mechanical interplay within engineered tissue. *Semin. Cell. Dev. Biol.* **2009**, *20*, 656-64. DOI
37. Guo, H.; Qiao, T.; Jiang, S.; et al. Aligned poly (glycolide-lactide) fiber membranes with conducting polypyrrole. *Polym. Adv. Technol.* **2016**, *28*, 484-90. DOI
38. Koons, G. L.; Diba, M.; Mikos, A. G. Materials design for bone-tissue engineering. *Nat. Rev. Mater.* **2020**, *5*, 584-603. DOI
39. Singhal, J. P.; Ray, A. R. Synthesis of blood compatible polyamide block copolymers. *Biomaterials* **2002**, *23*, 1139-45. DOI
40. Ince Yardimci, A.; Aypek, H.; Ozturk, O.; et al. CNT Incorporated Polyacrilonitrile/Polypyrrole Nanofibers as Keratinocytes Scaffold. *JBBBE.* **2019**, *41*, 69-81. DOI
41. Zhao, X.; Wu, H.; Guo, B.; Dong, R.; Qiu, Y.; Ma, P. X. Antibacterial anti-oxidant electroactive injectable hydrogel as self-healing wound dressing with hemostasis and adhesiveness for cutaneous wound healing. *Biomaterials* **2017**, *122*, 34-47. DOI
42. Fahlgren, A.; Bratengeier, C.; Gelmi, A.; et al. Biocompatibility of polypyrrole with human primary osteoblasts and the effect of dopants. *PLoS. ONE.* **2015**, *10*, e0134023. DOI PubMed PMC
43. Chen, C.; Tsai, C.; Wu, P.; Wang, I.; Yu, J.; Tsai, W. Modulation of neural differentiation through submicron-grooved topography surface with modified polydopamine. *ACS. Appl. Bio. Mater.* **2018**, *2*, 205-16. DOI
44. Wang, L.; Wu, Y.; Hu, T.; Ma, P. X.; Guo, B. Aligned conductive core-shell biomimetic scaffolds based on nanofiber yarns/hydrogel for enhanced 3D neurite outgrowth alignment and elongation. *Acta. Biomater.* **2019**, *96*, 175-87. DOI
45. Lee, S. Y.; Kozalakis, K.; Baftizadeh, F.; et al. Cell-class-specific electric field entrainment of neural activity. *Neuron* **2024**, *112*, 2614-2630.e5. DOI PubMed PMC
46. Toth, A. B.; Shum, A. K.; Prakriya, M. Regulation of neurogenesis by calcium signaling. *Cell. Calcium.* **2016**, *59*, 124-34. DOI PubMed PMC
47. Hao, B.; Webb, S. E.; Miller, A. L.; Yue, J. The role of Ca^{2+} signaling on the self-renewal and neural differentiation of embryonic stem cells (ESCs). *Cell. Calcium.* **2016**, *59*, 67-74. DOI
48. Yang, Y.; Sun, J.; Liu, X.; et al. Wet-spinning fabrication of shear-patterned alginate hydrogel microfibers and the guidance of cell alignment. *Regen. Biomater.* **2017**, *4*, 299-307. DOI PubMed PMC
49. Borges, M. H.; Nagay, B. E.; Costa, R. C.; Souza, J. G. S.; Mathew, M. T.; Barão, V. A. Recent advances of polypyrrole conducting polymer film for biomedical application: Toward a viable platform for cell-microbial interactions. *Adv. Colloid. Interface. Sci.* **2023**, *314*, 102860. DOI
50. Wang, P.; You, J.; Liu, G.; et al. The combination of aligned PDA-Fe@PLCL conduit with aligned GelMA hydrogel promotes peripheral nerve regeneration. *Adv. Healthc. Mater.* **2024**, *14*, 2403370. DOI
51. Jin, S.; Jung, H.; Song, J.; et al. Adhesive and conductive fibrous hydrogel bandages for effective peripheral nerve regeneration. *Adv. Healthc. Mater.* **2025**, *14*, 2403722. DOI